

Additive biomass models for *Larix* spp. single-trees sensitive to temperature and precipitation in Eurasia

Vladimir A. Usoltsev^{1,2}, Walery Zukow^{3*}, Anna A. Osmirko¹, Ivan S. Tsepordey²,
Viktor P. Chasovskikh¹

¹Ural State Forest Engineering University Sibirskii trakt 37, Yekaterinburg,
620100 Russian Federation

²Botanical Garden, Russian Academy of Sciences, Ural Branch, 8 Marta 202a,
Yekaterinburg, 620144 Russian Federation

³ Department of Spatial Management and Tourism, Faculty of Earth Sciences,
Nicolaus Copernicus University, Lwowska 1, 87-100 Toruń, Poland,
*e-mail: w.zukow@wp.pl

Received: 12 November 2018 / Accepted: 14 March 2019

Abstract. The analysis of the biomass of larch (genus *Larix* spp.) trees on the total component composition based on regression equations having the additive biomass structure. Two trends of changes in the tree biomass structure are revealed: due to the mean January temperature and due to the mean annual precipitation.

It was shown for the first time that both trends are mutually determined: the intensity of biomass trend in relation to the temperature is changing when depending on the level of precipitation, and the intensity of biomass trend in relation to precipitation level is changing during to a transition from the cold zone to the warm one and vice versa.

Key words: larch trees, biosphere role of forests, tree biomass, allometric models, additive biomass equations, mean January temperature, mean annual precipitation.

1. Introduction

International commitments to reduce CO₂ emissions and to prevent the mean annual temperature from rising by more than 2°C by the end of the century can be realized, in particular, by increasing the biomass stock in the vegetation cover by means of effective forest management. Allometric equations designed to estimate biomass and its dynamics in forest-covered areas in relation to a particular tree species, sensitive to changes in climatic parameters such as temperature and precipitation, are presented by single studies (Forrester et al., 2017; Zeng et al., 2017).

Attempt to explain some intra - and interspecific variability of different biomass components of equal-sized trees using the data of 27 tree species of Europe on the basis of allometrical models with the involvement of such additional independent variables as age, basal area and tree density, as well as mean annual temperature and precipitation, showed the influence of these additional variables, including temperature and precipitation, were statistically not significant for all the components (Forrester et al., 2017). The latter phenomenon may be explained by small temperature and precipitation ranges within Europe.

A unique result was obtained in China, where an allometric model, including the stem diameter and height

as independent variables, was developed for above- and underground biomass of 600 sample trees of eight larch species (genus *Larix* spp.) growing throughout this vast country. After introduction into the allometric model indices of the mean annual temperature and precipitation, as additional independent variables, it is established that the temperature increase by 1°C leads to an increase in the aboveground biomass of equal-sized trees by 0.9% and to a decrease in the underground one by 2.3%, and an increase in precipitation by 100 mm causes a decrease in the above- and underground phytomass by 1.5 and 1.1%, respectively (Zeng et al., 2017).

Today, for the main tree species in North America, Europe and Japan, there are, respectively, about 2600, 970 and 1000 allometric equations for biomass estimates mainly using tree height and stem diameter as independent variables (Jenkins et al., 2004; Forrester et al., 2017; Hosoda & Iehara, 2010). Such equations usually have a local or regional level, but in recent years, estimates of forest biomass have reached the global level, the Big Data Era (<http://www.gfbinitiative.org/symposium2017>) coming is stated, and global regularities of biological productivity of

forests and their constituent trees are derived at the level of mathematical models using such “Big Data” (Poorter et al., 2015; Liang et al., 2016; Jucker et al., 2017).

All above mentioned models are internally contradictory, they are not harmonized by the biomass structure, i.e. they do not provide the additivity of component composition, according to which the total biomass of components (stems, branches, needles, roots) obtained by «component» equations would be equal to the value of biomass obtained by the total biomass equation (Dong et al., 2015). The influence of climatic changes on the biomass of a particular tree species in the format of additive models according to transcontinental hydrothermal gradients has not been studied at all.

In the present study, the first attempt is made to simulate the changes in the additive component composition of tree biomass in larch forests on Trans-Eurasian hydrothermal gradients. In the simulation we used the database of the biomass of 520 sample trees (genus *Larix* spp.), the distribution of sample plots of which in the territory of Eurasia is shown in Figure 1 (Usoltsev, 2016).

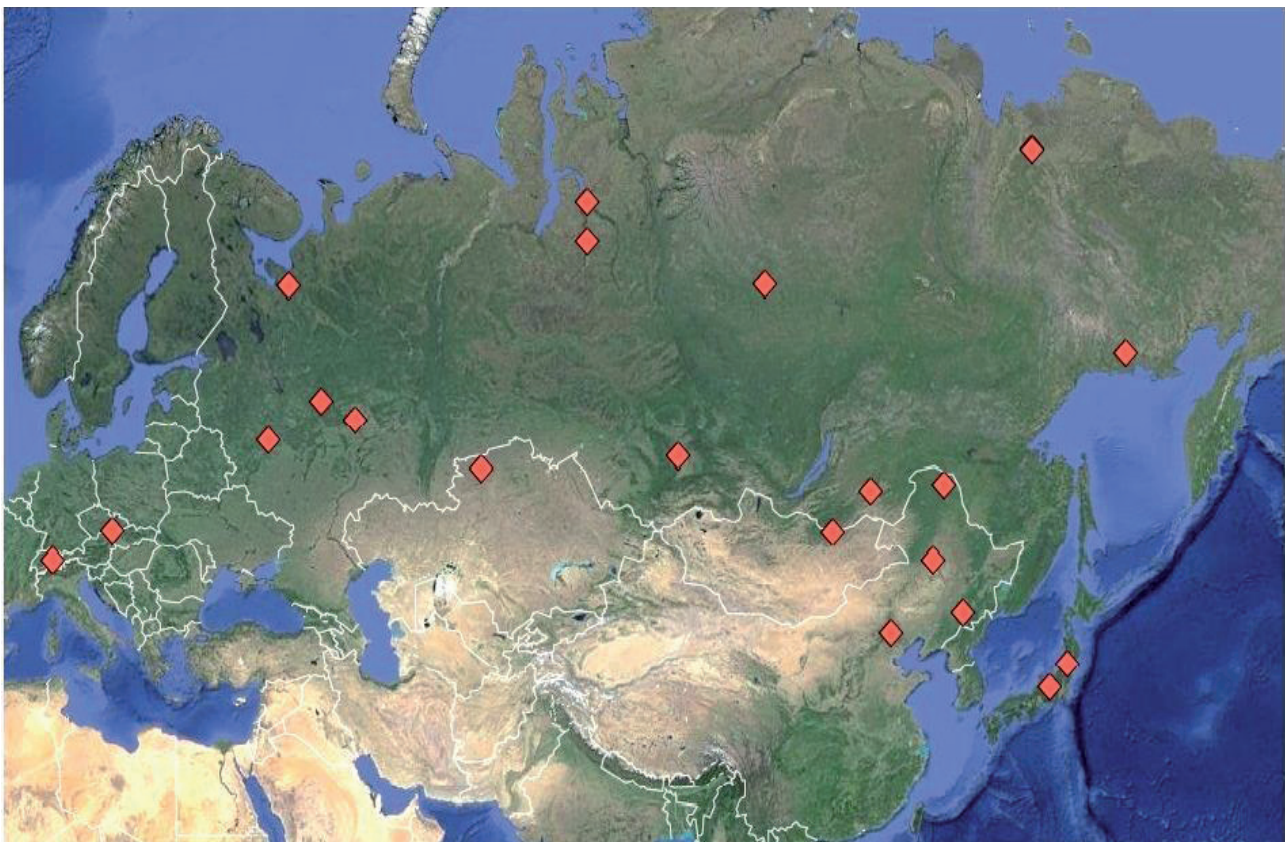


Figure 1. Distribution of sample plots with biomass measurements (kg) of 520 model larch trees on the territory of Eurasia

2. Materials and methods

Of the 520 sample trees described in the above-mentioned database containing data on biomass and dendrometric parameters, 420 trees were selected for the analysis, including six species of the genus *Larix* spp. Their distribution by regions, tree species and mensuration indices is presented in Table 1. One hundred trees from the database were omitted in our analysis due to the lack of height measurements.

Each sample plot on which tree biomass estimating was performed is positioned relatively to the isolines of the mean January temperature (Fig. 2) and relatively to the isolines of mean annual precipitation (Fig. 3). The matrix of harvest data was compiled, in which the biomass component values and mensuration tree parameters were related with the corresponding values of mean January temperature and precipitation, then included in the regression analysis procedure.

Table 1. Distribution of the 420 larch sample trees by regions, tree species and mensuration indices

Regions	Species of the genus <i>Larix</i> spp.*	Ranges:			Data number
		ages, yrs	diameters, cm	heights, m	
West Europa	<i>L. decidua</i> Mill.	34÷210	7.1÷47.8	9.8÷34.0	19
European Russia	<i>L. sukaczewii</i> Dylis	10÷70	1.0÷35.0	2.3÷28.0	25
Turgay deflection	<i>L. sukaczewii</i> Dylis	26÷42	6.2÷28.0	7.9÷17.8	28
North of West Siberia	<i>L. sibirica</i> Ledeb. <i>L. gmelinii</i> (Rupr.) Kuzen	10÷70	2.1÷38.0	2.9÷24.8	116
North of Eastern Siberia	<i>L. cajanderi</i> Mayr	44÷400	0.3÷22.7	1.4÷14.8	66
North of Russian Far East	<i>L. cajanderi</i> Mayr	30÷424	3.9÷52.8	2.9÷30.0	43
Mongolia. China	<i>L. sibirica</i> Ledeb. <i>L. gmelinii</i> (Rupr.) Kuzen.	14÷186	0.5÷31.0	1.5÷24.3	50
Japan	<i>L. leptolepis</i> (Siebold & Zucc.) Gordon	9÷56	4.0÷35.9	4.3÷26.7	73

* according to The Plant List (2019) *Larix sukaczewii* Dylis is a synonym of *L. sibirica* Ledeb.; *L. decidua* Mill. subsp. *sibirica* (Ledeb.) Domin = *L. sibirica* Ledeb.; *L. cajanderi* Mayr is a synonym of *L. gmelinii* (Rupr.) Kuzen.; and *L. leptolepis* (Siebold & Zucc.) Gordon = *L. kaempferi* (Lamb.) Carrière.

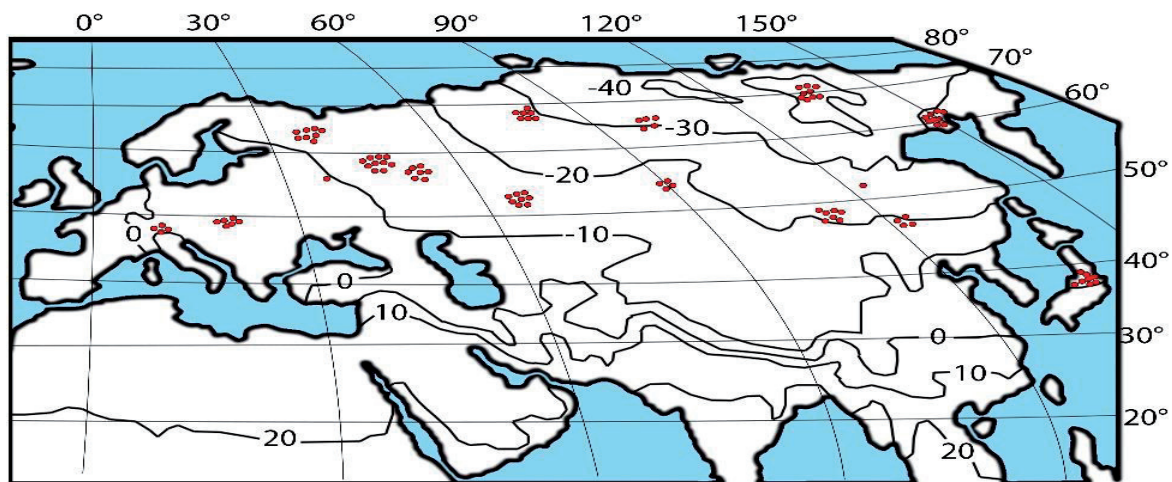


Figure 2. Distribution of biomass harvest data of 420 larch sample trees on the map of the mean January temperature, °C (World Weather Maps, 2007)

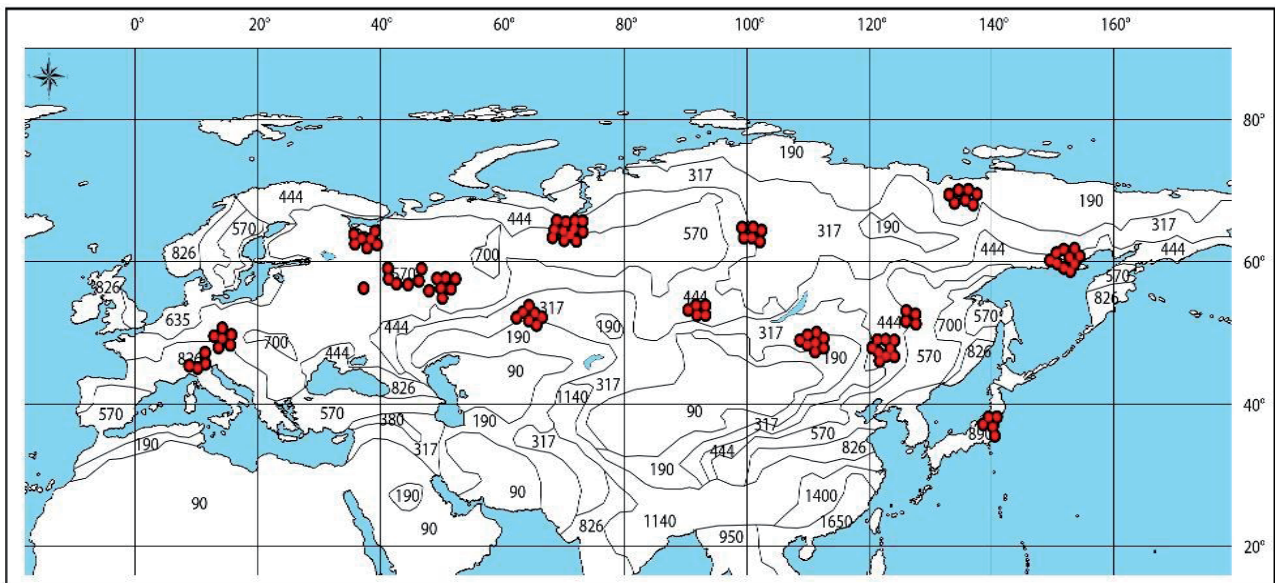


Figure 3. Distribution of biomass harvest data of 420 larch sample trees on the map of the mean annual precipitation, mm (World Weather Maps, 2007)

As noted above, the main predictors included in allometric biomass models are usually the stem diameter and height. The same two indices were used in the development of the Trans-Eurasian additive model of *Larix* spp. tree biomass, localized in the ecoregions using the dummy variables and having a purpose of drawing up the regional mensuration tables (Usoltsev et al., 2018a; Usoltsev et al., 2018b). In the calculation of allometric models of tree biomass there is always some residual variance, reflecting, in particular, the mismatch between the dynamic mass of the crown, especially of needles, and discrete accounting the relatively stable values of tree diameter and height (Usoltsev, 1988), as well as differences in age, soil and climatic conditions. In this study, the task is to extract a climatic component from the residual dispersion obtained in the calculation of a biomass model involving tree mensuration indices. To pre-dominate the share of climatic factors in this “information noise”, it is necessary to take into account in the model in addition to the diameter and height also the age of a tree, which is a factor largely determining the structure of its biomass (Nikitin, 1965).

A negative relationship between the crown biomass of equal-sized trees and their age in forest stands is well known. Thus, the crown mass of the tree with a diameter of 12 cm at the age of 15 years exceeds that at the age of 35 years at the birch by 1.5-2.0 times, and at the aspen – by 2.4-4.4 times (Usoltsev, 1972) due to the age shift of the cenotic position of equal-sized trees: at the age of 15 years such tree is the leader, and at the age of 35 years it is the depressed tree, a candidate for dying. Tree age, all

other conditions being equal, also affects the mass of roots in terms of root-leaf relationships (Kazaryan, 1969). The influence of age on stem biomass in comparison with other components is minimal due to the relative stability of the stem shape: with the same stem shape and the corresponding volume, its biomass changes with age only due to age-related changes in the basic density related to a decrease in the proportion of sapwood having a reduced dry matter content compared to the heartwood. Thus, in the Turgay deflection pine forests, the basic density of stems in the age ranging from 10 to 100 years increases from 490 to 580 kg/m³ (Usoltsev, 1988).

According to the structure of the disaggregation model of a three-step additive equation system (Tang et al., 2000; Dong et al., 2015), the total biomass P_p , estimated by the initial equation, is divided into component biomass estimated by corresponding equations according to the scheme presented in Figure 4 and Table 2.

3. Results

Initial regression equations are calculated

$$\ln P_i = a_{0i} + a_{1i}(\ln A) + a_{2i}(\ln D) + a_{3i}(\ln H) + a_{4i}(\ln D)(\ln H) + a_{5i}[\ln(T+50)] + a_{6i}(\ln PR), \quad (1)$$

where P_i is biomass of i -th component, kg; A is tree age, yrs; D and H are stem diameter (cm) at breast height and tree height (m), correspondingly; i is the index of biomass

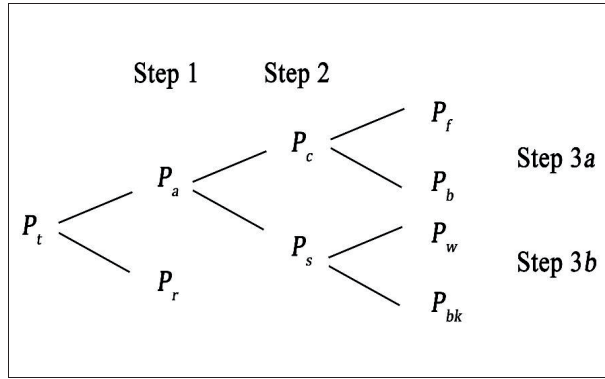


Figure 4. The pattern of disaggregating three-step proportional weighting additive model. Designation: $P_t, P_a, P_r, P_c, P_s, P_f, P_b, P_w$ and P_{bk} are tree biomass respectively: total, underground (roots), aboveground, crown (foliage and branches), stems above bark (wood and bark), foliage, branches, stem wood and stem bark correspondingly, kg

component: total (t), aboveground (a), roots (r), crown (c), stem above bark (s), foliage (f), branches (b), stem wood (w) and stem bark (bk); T is mean January temperature, °C; PR is mean annual precipitation, mm. The schematic map of the isolines of mean January temperature, rather than the mean annual temperature, is used, since climate warming is most pronounced in the cold half of the year (Golubiatnikov & Denisenko, 2009; Laing & Binyamin, 2013).

Since the mean January temperature in the northern part of Eurasia has negative values, the corresponding independent variable is modified to the form $(T+50)$ which may be subjected to logarithmic procedure. Along with the two main mass-forming tree indices – stem diameter D and height H – the product of variables $(\ln D)(\ln H)$ is introduced as an additional predictor, the need for which is obvious in Figure 5 (Usoltsev et al., 2017).

Characteristic of equations (1) is obtained by regression analysis, and after correcting on logarithmic transformation by G. L. Baskerville (1972) and anti-log transforming is given in the Table 3. Equations (1) are characterized by the significance level of not lower than 0.05. By introducing the original (initial) equations from the Table 3 into the additive scheme shown in the Table 2, the final model is obtained (Table 4).

Since it was established (Cunia & Briggs, 1984; Reed & Green, 1985) that the elimination of the internal inconsistency of biomass equations by ensuring their additivity does not necessarily means the increase in the accuracy of its estimates, it is necessary to clarify whether the obtained additive model is adequate enough and how its characteristics relate to the indices of the adequacy of initial equations? For this purpose both the additive model (see Table 4) and the initial equations (see Table 3), are tabu-

Table 2. The structure of the three-step additive model, sold under proportional weighting when using 122 sample trees of *Larix gmelinii* Rupr. (Dong et al., 2015). Symbols here and further as per equation (1)

Step 1	$P_a = \frac{1}{1 + \frac{a_r D^{b_r} H^{c_r}}{a_a D^{b_a} H^{c_a}}} \times P_t$	$P_r = \frac{1}{1 + \frac{a_a D^{b_a} H^{c_a}}{a_r D^{b_r} H^{c_r}}} \times P_t$
Step 2	$P_c = \frac{1}{1 + \frac{a_s D^{b_s} H^{c_s}}{a_c D^{b_c} H^{c_c}}} \times P_a$	$P_s = \frac{1}{1 + \frac{a_c D^{b_c} H^{c_c}}{a_s D^{b_s} H^{c_s}}} \times P_a$
Step 3a	$P_f = \frac{1}{1 + \frac{a_b D^{b_b} H^{c_b}}{a_f D^{b_f} H^{c_f}}} \times P_c$	$P_b = \frac{1}{1 + \frac{a_f D^{b_f} H^{c_f}}{a_b D^{b_b} H^{c_b}}} \times P_c$
Step 3b	$P_w = \frac{1}{1 + \frac{a_{bk} D^{b_{bk}} H^{c_{bk}}}{a_w D^{b_w} H^{c_w}}} \times P_s$	$P_{bk} = \frac{1}{1 + \frac{a_w D^{b_w} H^{c_w}}{a_{bk} D^{b_{bk}} H^{c_{bk}}}} \times P_s$

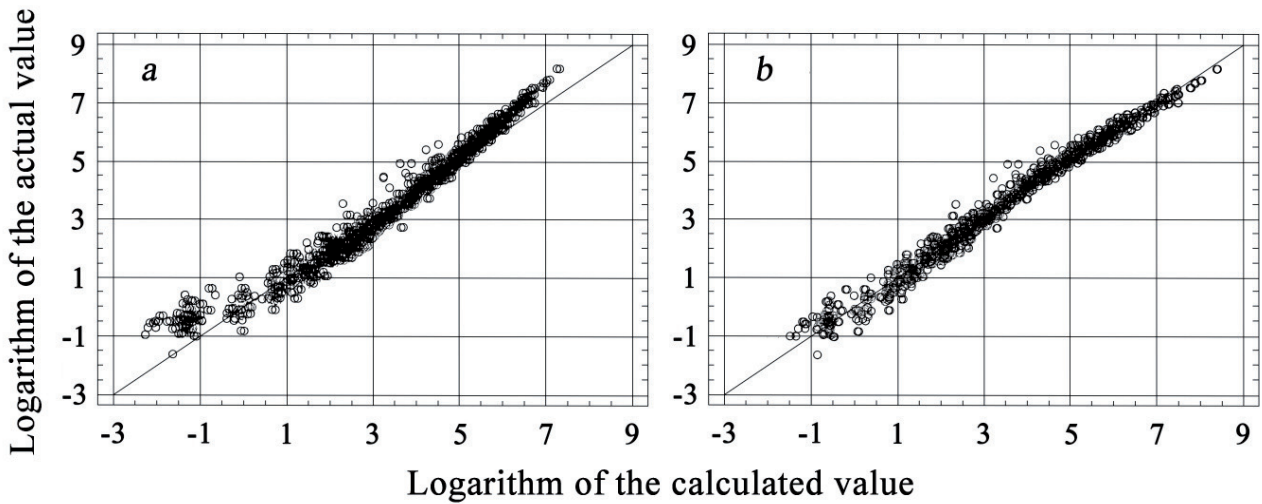


Figure 5. Graphical visual confirmation of the heterogeneity of the residual dispersion (a) and its absence after the introduction of the synergism $(\ln D)(\ln H)$ (b) into Equation (1)

lated on the experimental mass-forming indices, and the obtained calculated biomass values are compared with the actual ones according to R^2 . The results of the comparison shown in the Table 5, indicate that the adequacy of the two systems of equations are close to each other. The ratio of harvest biomass data and values obtained by the calculation of initial and additive models of tree biomass (Figure 6), shows the degree of correlation of these values and the absence of visible differences in the structure of residual dispersions obtained from the two models.

Due to the many times greater complexity of measuring the tree height compared to the stem diameter one uses specially designed equations or tables that reflect the relationship of the height of trees to the tree age and the stem diameter. For this purpose, a recursive system of equations (2) and (3) for mass-forming indices is calculated

$$\begin{aligned}
 A &= \exp\{4.3909+0.5813(\ln D)-1.4129[\ln(T+50)]+ \\
 &\quad +0.4764(\ln PR)\}; \quad adjR^2=0.600; \quad SE = 1.64 \quad (2); \\
 H &= \exp\{0.00023+0.0135(\ln A)+0.6479(\ln D)+ \\
 &\quad +0.1915[\ln(T+50)]+0.0241(\ln PR)\}; \\
 &\quad adjR^2 = 0.901; \quad SE = 1.20. \quad (3)
 \end{aligned}$$

Since the tabulation of equations (1) using the given values A , D , H , T and PR results in a too cumbersome table, the required figures of the tree biomass dependence upon temperature T and precipitation PR are constructed as a fragment for trees having the age A equal 100 years, diameter D equal 24 cm and tree height H equal 22 m (Figure 7).

4. Discussion

Configuration of the surfaces obtained in three-dimensional space in Figure 5 allows to draw some nontrivial conclusions. Thus, in the cold zone ($T = -40^\circ\text{C}$) when increasing precipitation, the aboveground phytomass, the mass of the trunk, needles and branches of larch trees decreases, and the underground mass increases. The trend of underground biomass is less pronounced in comparison with that of aboveground one, and as a result, the total biomass of trees, as well as aboveground with its components, decreases with increasing precipitation.

In the warm zone ($T = 0^\circ\text{C}$) the opposite regularities of changes in the above- and underground biomass are remained, but both are expressed very weakly in comparison with the cold zone. At the same time, the decrease in aboveground biomass with increasing precipitation is due to the stem biomass, since the needles and branches biomass in the warm belt practically does not react to precipitation.

In regions with low precipitation level ($PR = 250$ mm), the above- and underground biomasses of trees, as well as the biomass of stems, needles and branches, are decreasing with the growth of air temperature, and in areas of high precipitation level ($PR = 800$ mm), the patterns of changes in the above- and underground biomass due to the increase in temperature are opposite: the aboveground biomass increases, and the underground one decreases. At the same time, the increase in the aboveground biomass is due to the stem biomass, since the biomass of needles and branches

Table 3. Characteristics of original model (1) after its anti-log transforming

Biomass components	The original model characteristics							$adjR^{2*}$	SE^*
P_t	7.79E-02	$A^{0.2062}$	$D^{1.6047}$	$H^{0.7393}$	$D^{0.0187(\ln t)}$	$(T+50)^{-0.2526}$	$PR^{0.1181}$	0.976	1.29
Step 1									
P_a	5.36E-01	$A^{-0.0346}$	$D^{1.4706}$	$H^{0.2555}$	$D^{0.1916(\ln t)}$	$(T+50)^{-0.1482}$	$PR^{-0.0934}$	0.989	1.21
P_r	8.20E-05	$A^{0.6252}$	$D^{2.2515}$	$H^{0.6089}$	$D^{-0.1684(\ln t)}$	$(T+50)^{-1.4032}$	$PR^{1.3380}$	0.899	1.86
Step 2									
P_c	5.11E+00	$A^{-0.4798}$	$D^{2.0900}$	$H^{-1.6683}$	$D^{0.3613(\ln t)}$	$(T+50)^{-0.5104}$	$PR^{0.0664}$	0.908	1.65
P_s	1.69E-01	$A^{0.03905}$	$D^{1.3685}$	$H^{0.7084}$	$D^{0.1473(\ln t)}$	$(T+50)^{-0.1038}$	$PR^{-0.1011}$	0.990	1.21
Step 3a									
P_f	5.45E+00	$A^{-0.5719}$	$D^{1.9789}$	$H^{-1.4711}$	$D^{0.3050(\ln t)}$	$(T+50)^{-0.5820}$	$PR^{-0.0740}$	0.880	1.67
P_b	2.59E+00	$A^{-0.4602}$	$D^{2.1997}$	$H^{-1.6854}$	$D^{0.3533(\ln t)}$	$(T+50)^{0.5039}$	$PR^{0.0919}$	0.907	1.69
Step 3b									
P_w	2.40E-01	$A^{0.0289}$	$D^{1.2728}$	$H^{0.8745}$	$D^{1.2728(\ln t)}$	$(T+50)^{-0.2002}$	$PR^{-0.1979}$	0.992	1.19
P_{bk}	6.96E-01	$A^{-0.0022}$	$D^{1.2203}$	$H^{0.5562}$	$D^{0.1691(\ln t)}$	$(T+50)^{-0.3025}$	$PR^{-0.4037}$	0.968	1.37

* $adjR^2$ – coefficient of determination adjusted for the number of parameters; SE – equation standard error.

Table 4. Final three-step additive model of tree biomass

	$P_t = 7.79E-02 A^{0.2062} D^{1.6047} H^{0.7393} D^{0.0187(\ln t)} (T+50)^{-0.2526} PR^{0.1181}$
Step 1	$P_a = \frac{1}{1 + 5.36E-01 A^{-0.0346} D^{1.4706} H^{0.2555} D^{0.1916(\ln t)} (T+50)^{-0.1482} PR^{-0.0934}} \times P_t$
	$P_r = \frac{1}{1 + 8.20E-05 A^{0.6252} D^{2.2515} H^{0.6089} D^{-0.1684(\ln t)} (T+50)^{-1.4032} PR^{1.3380}} \times P_t$
Step 2	$P_c = \frac{1}{1 + 5.11E+00 A^{-0.4798} D^{2.0900} H^{-1.6683} D^{0.3613(\ln t)} (T+50)^{-0.5104} PR^{0.0664}} \times P_a$
	$P_s = \frac{1}{1 + 1.69E-01 A^{0.03905} D^{1.3685} H^{0.7084} D^{0.1473(\ln t)} (T+50)^{-0.1038} PR^{-0.1011}} \times P_a$
Step 3a	$P_f = \frac{1}{1 + 5.45E+00 A^{-0.5719} D^{1.9789} H^{-1.4711} D^{0.3050(\ln t)} (T+50)^{-0.5820} PR^{-0.0740}} \times P_c$
	$P_b = \frac{1}{1 + 2.59E+00 A^{-0.4602} D^{2.1997} H^{-1.6854} D^{0.3533(\ln t)} (T+50)^{0.5039} PR^{0.0919}} \times P_c$
Step 3b	$P_w = \frac{1}{1 + 2.40E-01 A^{0.0289} D^{1.2728} H^{0.8745} D^{1.2728(\ln t)} (T+50)^{-0.2002} PR^{-0.1979}} \times P_s$
	$P_{bk} = \frac{1}{1 + 6.96E-01 A^{-0.0022} D^{1.2203} H^{0.5562} D^{0.1691(\ln t)} (T+50)^{-0.3025} PR^{-0.4037}} \times P_s$

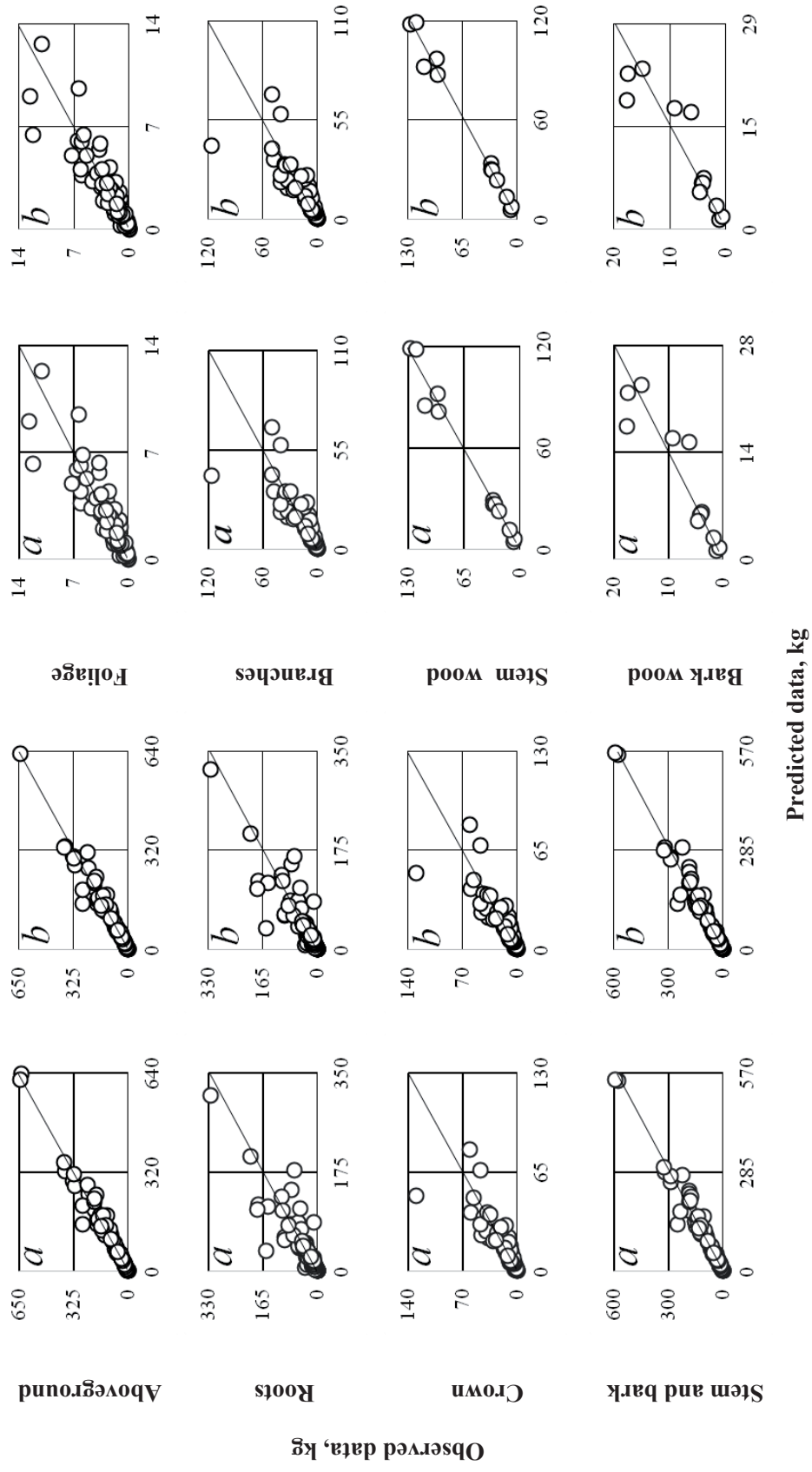


Figure 6. The ratio of the harvest biomass and its values obtained by calculating the initial (a) and additive (b) models of the larch tree biomass

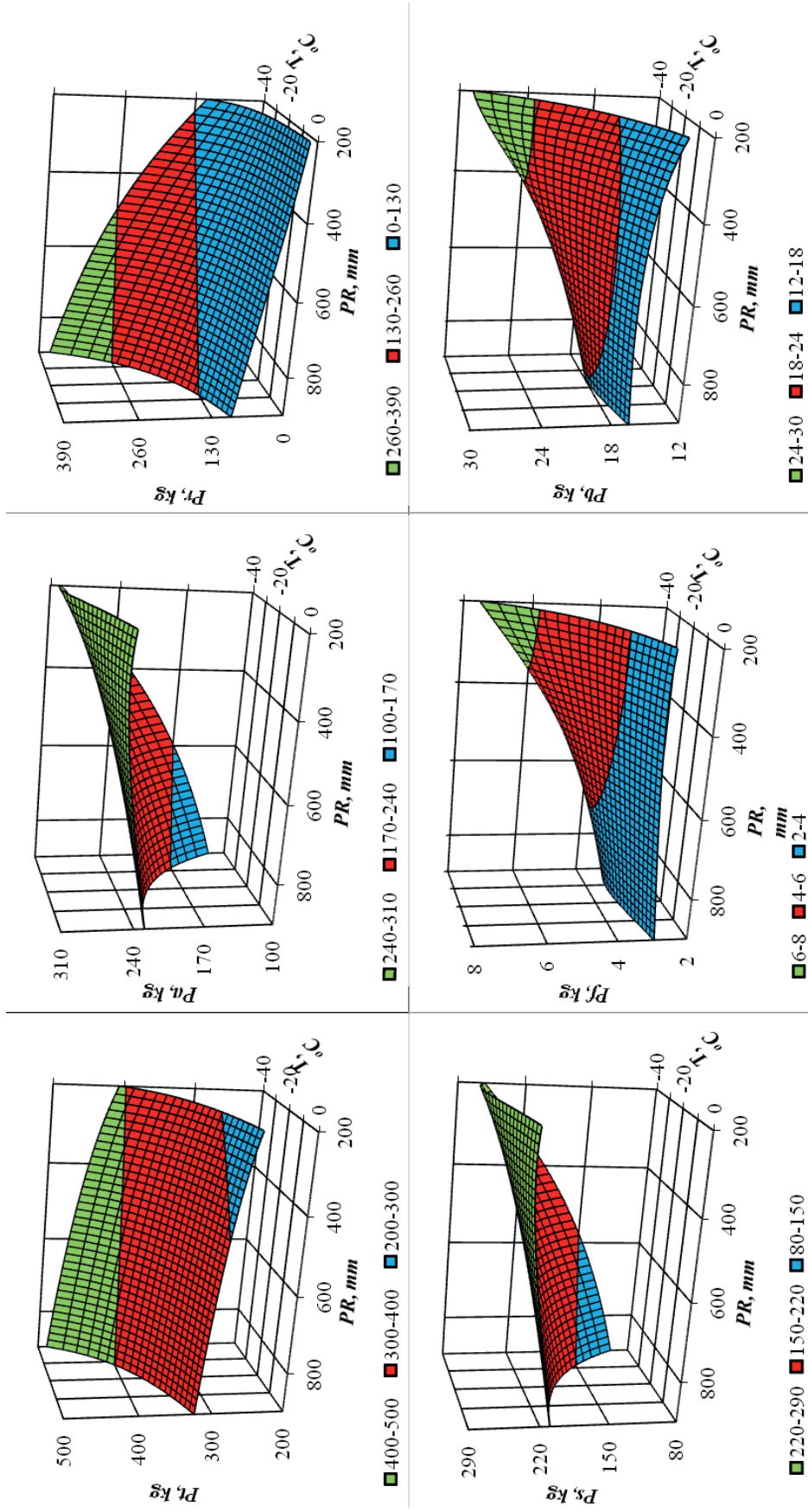


Figure 7. Dependence of larch tree biomass upon the January mean temperature (T) and precipitation (PR). Designations: P_t , P_s , P_a , P_f , P_r and P_b are correspondingly biomass: total, stems, aboveground, foliage, roots and branches, kg

Table 5. Comparison of coefficients of determination of the initial and additive equations of larch tree biomass

Biomass components								
P_t	P_a	P_r	P_s	P_w	P_{bk}	P_c	P_b	P_f
Initial equations								
0.824	0.969	0.767	0.965	0.959	0.481	0.686	0.647	0.807
Additive equations								
0.824	0.964	0.781	0.962	0.978	0.358	0.685	0.644	0.815

practically does not react to temperature changes in conditions of precipitation level.

The obtained additive models of larch tree biomass make it possible to establish quantitative changes in the structure of tree biomass due to climatic changes, in particular, the mean temperature of January and mean annual precipitation.

5. Conclusions

Thus, the first our attempt to model changes in additive component composition of the biomass of larch trees on the Trans-Eurasian hydrothermal gradients revealed the presence of nontrivial patterns. As it was noted above, two main regularities of the change of biomass of larch trees in China were obtained: (1) depending on the mean temperature without taking into account any changes in humidity and (2) depending on the mean annual precipitation without taking into account changes in temperature. At the same time, the aboveground biomass was not subdivided into components, and the system of equations was not additive.

Two trends of changes in the tree biomass structure are revealed in our study: due to the mean January temperature and due to the mean annual precipitation. It was shown for the first time that both trends are mutually determined: the intensity of biomass trend in relation to the temperature is changing when depending on the level of precipitation, and the intensity of biomass trend in relation to precipitation level is changing during to a transition from the cold zone to the warm one and vice versa. The adequacy of the obtained regularities is determined by the level of variability explained by the proposed regression models (88-99 %).

The results mentioned are preliminary because, as can be seen in Figures 1, 2 and 3, the proposed models did not take into account most of the territory of China, for which there are, as was shown above, the data on the biomass structure of 600 sample trees. More correct regularities of larch tree biomass changes in hydrothermal gradients throughout Eurasia, including China, can be obtained from the total quantity of 1020 sample trees.

The development of such models for the main forest-forming species of Eurasia will make it possible to predict changes in the productivity of the forest cover of Eurasia in relation to climate change.

References

- Baskerville G.L., 1972, Use of logarithmic regression in the estimation of plant biomass. *Canadian Journal of Forest Research* 2: 49-53.
- Cunia T. & Briggs R.D., 1984, Forcing additivity of biomass tables: some empirical results. *Canadian Journal of Forest Research* 14: 376-384.
- Dong L., Zhang L. & Li F., 2015, A three-step proportional weighting system of nonlinear biomass equations. *Forest Science* 61(1): 35-45.
- Forrester D.I., Tachauer I.H.H., Annighoefer P., Barbeito I., Pretzsch H., Ruiz-Peinado R., Stark H., Vacchiano G., Zlatanov T., Chakraborty T., Saha S. & Silési G.W., 2017, Generalized biomass and leaf area allometric equations for European tree species incorporating stand structure, tree age and climate. *Forest Ecology and Management* 396: 160-175.
- Golubyatnikov L.L. & Denisenko E.A., 2009, Influence of climatic changes on the vegetation of European Russia. *News of Russian Academy of Sciences. Geographic series* 2: 57-68.
- Hosoda K. & Iehara T., 2010, Aboveground biomass equations for individual trees of *Cryptomeria japonica*, *Chamaecyparis obtusa* and *Larix kaempferi* in Japan. *J. For. Res.* 15(5): 299-306. (doi: 10.1007/s10310-010-0192-y).
- Jenkins J.C., Chojnacky D.C., Heath L.S. & Birdsey R.A., 2004, Comprehensive database of diameter-based regressions for North American tree species. USDA Forest Service Northeastern Research Station. General Technical Report NE-319. 45 pp.
- Jucker T., Caspersen J., Chave J., Antin C., Barbier N., Bongers F., Dalponte M., van Ewijk K.Y., Forrester D.I., Heani M., Higgins S.I., Holdaway R.J., Iida Y., Lorimer C., Marshall P.M., Momo S., Moncrieff G.R.,

- Ploton P., Poorter L., Rahman K.A., Schlund M., Sonké B., Sterck F.J., Trugman A.T., Usoltsev V.A., Vanderwel M.C., Waldner P., Wedeux B., Wirth C., Wöll H., Woods M., Xiang W., Zimmermann N. & Coomes D.A., 2017, Allometric equations for integrating remote sensing imagery into forest monitoring programmes. *Global Change Biology* 23: 177-190.
- Kazaryan V.O., 1969, Aging of higher plants. Nauka Publ., Moscow.
- Laing J., & Binyamin J., 2013, Climate change effect on winter temperature and precipitation of Yellowknife, Northwest Territories, Canada from 1943 to 2011. *American Journal of Climate Change* 2: 275-283. (doi: 10.4236/ajcc.2013.24027).
- Liang J., Crowther T.W., Picard N., Wiser S., Zhou M., Alberti G., Schulze E.-D., McGuire A.D., Bozzato F., Pretzsch H., de-Miguel S., Paquette A., Hérault B., Scherer-Lorenzen M., Barrett C.B., Glick H.B., Hengeveld G.M., Nabuurs G.-J., Pfautsch S., Viana H., Vibrans A.C., Ammer C., Schall P., Verbyla D., Tchebakova N.M., Fischer M., Watson J.V., Chen H.Y.H., Lei X., Schelhaas M.-J., Lu H., Gianelle D., Parfenova E.I., Salas C., Lee E., Lee B., Kim H.S., Bruelheide H., Coomes D.A., Piotta D., Sunderland T., Schmid B., Gourlet-Fleury S., Sonké B., Tavani R., Zhu J., Brandl S., Vayreda J., Kitahara F., Searle E.B., Neldner V.J., Ngugi M.R., Baraloto C., Frizzera L., Balazy R., Oleksyn J., Zawila-Niedzwiecki T., Bouriaud O., Bussotti F., Finér L., Jaroszewicz B., Jucker T., Valladares F., Jagodzinski A.M., Peri P.L., Gonmadje C., Marthy W., O'Brien T., Martin E.H., Marshall A.R., Rovero F., Bitariho R., Niklaus P.A., Alvarez-Loayza P., Chamuya N., Valencia R., Mortier F., Wortel V., Engone-Obiang N.L., Ferreira L.V., Odeke D.E., Vasquez R.M., Lewis S.L. & Reich P.B., 2016, Positive biodiversity-productivity relationship predominant in global forests. *Science* 354(6309): 196-208.
- Nikitin K.E., 1965, Forest and mathematics. *Lesnoe Khozyaistvo* [Forest Management] 5: 25-29.
- Poorter H., Jagodzinski A.M., Ruiz-Peinado R., Kuyah S., Luo Y., Oleksyn J., Usoltsev V.A., Buckley T.N., Reich P.B. & Sack L., 2015, How does biomass allocation change with size and differ among species? An analysis for 1200 plant species from five continents. *New Phytologist* 208(3): 736-749.
- Reed D.D. & Green E.J., 1985, A method of forcing additivity of biomass tables when using nonlinear models. *Canadian Journal of Forest Research* 15: 1184-1187.
- Tang S., Zhang H. & Xu H., 2000, Study on establish and estimate method of compatible biomass model. *Scientia Silvae Sinica* 36: 19-27. (in Chinese with English abstract).
- The Plant List, 2019, version 1.1. (<http://www.theplantlist.org>), [Accessed 12.03.2019].
- Usoltsev V.A., 1972, Birch and aspen crown biomass in forests of Northern Kazakhstan. *Vestnik Selskokhozyaistvennoi Nauki Kazakhstana* [Bulletin of Agricultural Science of Kazakhstan] 4: 77-80.
- Usoltsev V.A., 1988, Growth and structure of forest stand biomass. Novosibirsk: Nauka Publ. 253 pp. (<http://elar.usfeu.ru/handle/123456789/3352>).
- Usoltsev V.A., 2016, Single-tree biomass of forest-forming species in Eurasia: database, climate-related geography, weight tables. Yekaterinburg: Ural State Forest Engineering University. 336 pp. (<http://elar.usfeu.ru/handle/123456789/5696>).
- Usoltsev V.A., Kolchin K.V. & Voronov M.P., 2017, Dummy variables and biases of allometric models when local estimating tree biomass (on an example of *Picea* L.). *Eco-Potencial* 1(17): 22-39. (<http://elar.usfeu.ru/bitstream/123456789/6502/1/eko-1702.pdf>).
- Usoltsev V.A., Shobairi S.O.R. & Chasovskikh V.P., 2018a, Geographic gradients of forest biomass of two needled pines on the territory of Eurasia. *Ecological Questions* 29(2): 9-17. (<http://dx.doi.org/10.12775/EQ.2018.012>).
- Usoltsev V.A., Tsepordey I.S., Chasovskikh V.P. & Osmirko A.A., 2018b, Additive regional models of tree and stand biomass for Eurasia. Message 1: Genus *Larix* spp. *Eco-Potencial* 2(22): 16-34. (http://elar.usfeu.ru/bitstream/123456789/7665/1/eko_2-18-04.pdf).
- World Weather Maps, 2007, URL. (<https://www.mapsof-world.com/referrals/weather>).
- Zeng W.S., Duo H.R., Lei X.D., Chen X.Y., Wang X.J., Pu Y. & Zou W.T., 2017, Individual tree biomass equations and growth models sensitive to climate variables for *Larix* spp. in China. *European Journal of Forest Research* 136(20): 233-249. (<https://doi.org/10.1007/s10342-017-1024-9>).